Essential Role of a Ca^{2+}-Selective, Store-Operated Current (I_{SOC}) in Endothelial Cell Permeability
Determinants of the Vascular Leak Site

Songwei Wu, Eugene A. Cioffi, Diego Alvarez, Sarah L. Sayner, Hairu Chen, Donna L. Cioffi, Judy King, Judy R. Creighton, Mary Townsley, Steven R. Goodman, Troy Stevens

Abstract—Store-operated calcium (SOC) entry is sufficient to disrupt the extra-alveolar, but not the alveolar, endothelial cell barrier. Mechanism(s) underlying such insensitivity to transitions in cytosolic calcium ($[Ca^{2+}]_i$) in microvascular endothelial cells are unknown. Depletion of stored Ca^{2+} activates a larger SOC entry response in extra-alveolar (pulmonary artery; PAECs) than alveolar (pulmonary microvascular; PMVECs) endothelial cells. In vivo permeation studies revealed that Ca^{2+} store depletion activates similar nonselective cationic conductances in PAECs and PMVECs, while only PAECs possess the calcium-selective, store-operated Ca^{2+} entry current, I_{SOC}. Pretreatment with the type 4 phosphodiesterase inhibitor, rolipram, abolished thapsigargin-activated I_{SOC} in PAECs, and revealed I_{SOC} in PMVECs. Rolipram pretreatment shifted the thapsigargin-induced fluid leak site from extra-alveolar to alveolar vessels in the intact pulmonary circulation. Thus, our results indicate I_{SOC} provides a $[Ca^{2+}]_i$ source that is needed to disrupt the endothelial cell barrier, and demonstrate that intracellular events controlling I_{SOC} activation coordinate the site-specific vascular response to inflammation. (*Circ Res*. 2005;96:856-863.)

Key Words: store-operated calcium entry ■ thapsigargin ■ rolipram ■ permeability ■ phosphodiesterase

Endothelium is remarkably diverse, with significant structural and functional heterogeneity apparent between organs, along vascular segments, and indeed, within immediately adjacent cells. Relatively little is known about how such diversity is maintained, and how site-specific responses are determined. Transitions in cytosolic calcium ($[Ca^{2+}]_i$) fulfill important signaling roles in endothelium, including the dynamic regulation of interendothelial cell gap formation that increases water, solute, and protein permeability. However, Ca^{2+} entry specifically through store-operated channels provides a $[Ca^{2+}]_i$ source that is sufficient to increase permeability across a subset of macrovascular, but not across microvascular, endothelial cells.[1–3] Similarly, activation of store-operated calcium (SOC) entry increases macrovascular but not microvascular endothelial cell permeability in the intact pulmonary circulation.[4,5] Although microvascular endothelial cells possess enhanced cell-cell adhesion compared with their macrovascular counterparts,[1,6] the mechanism for their relative insensitivity to rises in $[Ca^{2+}]_i$ are not known.

We previously reported that the activation of SOC entry results in a smaller $[Ca^{2+}]_i$ transition in pulmonary microvascular endothelial cells (PMVECs) than in pulmonary artery endothelial cells (PAECs).[7] A more depolarized membrane potential, increased Ca^{2+} extrusion, or decreased Ca^{2+} entry could all account for the decreased PMVEC $[Ca^{2+}]_i$ response to thapsigargin. Evidence among different cell types illustrates that thapsigargin activates multiple ion channels, which differ in their biophysical characteristics, including ion selectivity.[8–10] For example, thapsigargin activates both Ca^{2+}-selective[11–15] and nonselective[16–18] cationic conductances in endothelial cells, although this work has routinely been performed using cells of conduit origin (eg, pulmonary artery, aorta, and human umbilical vein) and not from the microcirculation. Therefore, it is not known whether thapsigargin activates similar Ca^{2+}-selective and nonselective conductances in PAECs and PMVECs.

There is reason to suggest that macro- and microvascular endothelial cells do not express similar ion channels, or similar regulatory mechanisms, based partly on their distinct phenotypes and functions. Functional differences between macro- and microvascular endothelial cells are evident early in development, and transmissible through mitotic divisions into adulthood.[19] Our present studies therefore sought to determine whether PAECs and PMVECs possess different SOC entry pathways and, further, to identify which Ca^{2+} entry pathway controls interendothelial cell gap formation.

Materials and Methods

Isolation and culture of rat lung endothelial† cells. Endothelial cells were isolated and cultured as described.[20]

In Vitro Fluorescence Measurements

All fluorescence measurements were conducted using an SLM-AMINCO Model 8100 high-resolution spectrofluorometer and a 10-mm pathlength cell at ≈23°C. Initial spectra bandwidth and wavelength calibrations were performed using an NIST-traceable fluorescence intensity set (Wilmad Glass; cat. no. 921-1). Excitation and emission spectra were acquired using a 4-nm bandpass throughout the optical paths, with a spectral scan rate of 0.95 nm·sec^{-1} and integration time 1.0 second, in a toggled-excitation mode (to minimize photobleaching).

In Vitro Fura-2 Dye and Cation Measurements

All solutions were prepared using analytical-grade reagents, in >18 MΩ quality Type I water. Divalent salts (cation 2 Cl$^-$; Be^{2+}, Mg^{2+}, Ca^{2+}, Sr^{2+}, Ba^{2+}) and LaCl$_3$ (Aldrich Chemical) solutions were prepared as 10 mmol/L solutions in 1 μmol/L pluronic acid containing K$^+$ Ringers buffer, both in the absence and presence of 100 nmol/L Ca^{2+}. Fura-2 pentasodium salt (Molecular Probes) was prepared as per instructions.

Molecular Modeling

Molecular mechanics, semiempirical, and ab initio calculations using Spartun '02 (Wavefunction, Inc) were performed on a Dell 8200 (2.4-GHz Pentium 4) computer. The restricted Hartree-Fock SCF ab initio calculations used the 6-31G(d) basis set, which includes polarization functions, recommended for the description of heavy atoms in medium/large sized systems. The 6-31G(d) basis set was used for the initial ground-state molecular structure optimization. The default grid option was chosen for numerical integration of matrix elements. The 6-31G(d) basis set involved a total of 242 electrons with 238 contracted Gaussian basis functions consisting of 744 primitive Gaussians. The optimized parent ab initio structure was used as a basis for all subsequent molecular mechanics and semiempirical calculations. For all models, C$_1$ symmetry was used throughout full optimization and subsequent frequency calculations. Analytical harmonic vibrational frequencies were computed for all structures to confirm that local minima on the potential energy surface had been found. PM3 (Parameterized Model, revision 3) semiempirical and MMFF94 (Merck Pharmaceutical Force Field) molecular mechanics calculations were compared as applicable in the metal-ion complexed species. For Be^{2+}, a tetrahedral binding complex association was used; for all other $^{2+}$ and $^{3+}$ cations, octahedral binding complex associations were assumed.

Cytosolic Cation Measurements

Cytosolic Ca^{2+} was estimated using fura 2/acetoxymethylester (Molecular Probes) according to methods previously described.[13,14,18,21]

Patch Clamp Electrophysiology

Conventional whole-cell voltage-clamp configuration was performed to measure transmembrane currents in single rat PAEC or PMVEC by the standard giga-seal patch-clamp technique, as described.[14,15]

TRPC4 Expression in Endothelial Cells

PMVEC monolayers were lysed in hypotonic buffer, and membrane/cytoskeleton fractions prepared via differential centrifugation and homogenization. These fractions were extracted in Triton X-100 detergent containing 100 mmol/L potassium iodide and centrifuged at 145 000*g* (50 minutes, 4°C) to yield an insoluble pellet and soluble supernatant. Pellet and supernatant samples were subjected to SDS-PAGE and transferred to nitrocellulose membranes. Membranes were rocked with primary antibody to TRPC4 (gift from M. Zhu, The Ohio State University, Columbus, Ohio) and horseradish peroxidase
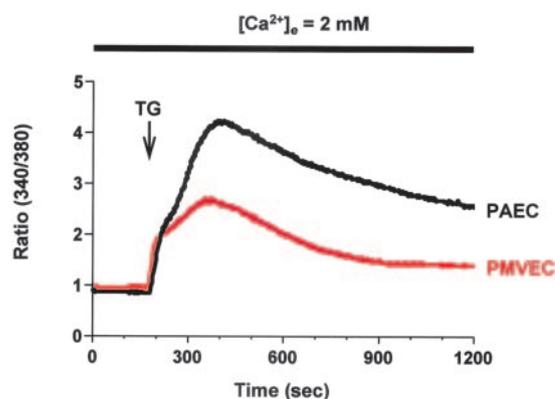

Figure 1. Activation of SOC entry elicits a larger [Ca^{2+}]$_i$ rise in PAECs than in PMVECs. Confluent cell monolayers were stimulated with thapsigargin (TG; 1 μmol/L). Thapsigargin induced a slowly developing rise in [Ca^{2+}]$_i$ that was sustained in both cell types, although the [Ca^{2+}]$_i$ response in PAECs was greater than it was in PMVECs. Representative trace shows results similar to those previously published elsewhere.[1,7]

tagged secondary antibody. Proteins were visualized via enhanced chemiluminescence detection.

Time-Lapse Microscopy

Cells were grown to confluence on 25-mm glass coverslips, placed on the microscope stage, and imaged (40× oil immersion) at 1-minute intervals for ≈2 hours using Metamorph and Spot Software (Diagnostic Instruments). Rolipram (10 μmol/L) was applied to monolayers for 16 minutes before application of thapsigargin (1 μmol/L), as indicated.[22]

Isolated Perfused Lung Experiments

Heart and lungs were removed en bloc from adult CD40 rats (≈300 to 400 g), suspended in a humidified environment, ventilated, and perfused as previously described.[22]

Methyl Methacrylate Casting Experiments

Lungs were isolated from anesthetized SD40 rats and endothelial permeability measured via Kf. Casting material was prepared as described by Gannon.[23] Methyl methacrylate was prepolymerized under UV light (312 nm) to achieve a viscosity of 2.4 cPs, a viscosity that has been shown to be optimal for identification of endothelial leaks.[4] After baseline measurements, lungs were treated for 20 minutes with either vehicle (DMSO 18 μL, n=4) or rolipram (10 μmol/L, n=3) followed by 20 minutes perfusion with thapsigargin (100 nmol/L), and a final Kf measured. Venous pressure was raised by ≈8 cm H$_2$O from baseline, and prepolymerized methyl methacrylate was combined with benzoyl peroxide, OH-propyl methacrylate, and *N-N'*-dimethyl aniline, and infused into the pulmonary circulation at a constant flow. After complete polymerization (≈1 hour after casting material infusion) successive corrosion of the lung casts was initiated and maintained over 3 weeks with alternating HCl and KOH (5 mol/L each). The casts were fragmented to expose the internal vascular architecture and specimens were mounted on aluminum stubs, coated with gold palladium, and examined using SEM (Philips XL 20, FEI). Pulmonary endothelial injury was determined by the appearance of blebs at the casting surface, which represent areas of endothelial leaks.[4]

Results

SOC Entry in PAECs and PMVECs

PAECs exhibit increased global [Ca^{2+}]$_i$ responses to thapsigargin when compared with PMVECs, although the mechanism accounting for this difference is not clear. Figure 1 demonstrates the typical [Ca^{2+}]$_i$ response to a near-maximal
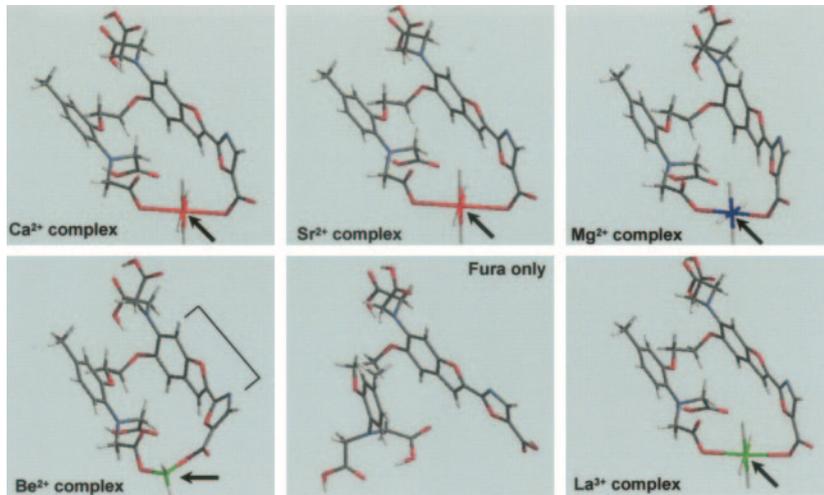
Figure 2. Parent Fura-2 and Fura-ion octahedral or tetrahedral complexes important for fluorescence detection. Fura-2 forms a distorted tetrahedral complex with Be^{2+} (see arrow), as seen by the 25.32° deviation from planarity in the oxazolyl- and benzofuranyloxy-π network (see bracket). Fura-2 forms octahedral complexes with Ca^{2+}, Mg^{2+}, Sr^{2+}, and La^{3+} (see arrow), with minimal deviation from planarity in the oxazolyl- and benzofuranyloxy-π network. Cation-complexed water molecules have been omitted for visual clarity.

thapsigargin (1 μmol/L; EC_{95}) concentration in both cell types, illustrating an $\approx$50% lower $[Ca^{2+}]_i$ rise in PMVECs.[7]

Thapsigargin activates a number of ion channels in endothelial cells, including channels that are selective and nonselective for Ca^{2+}.[18] Recently, Zweifach[24] developed a fura-based approach to evaluate ion permeability through SOC entry channels, using the recalcification protocol, allowing for discrimination between Ca^{2+}-selective and nonselective channels in living cells. To ascertain cation-induced influx in living cells, cation-fura interactions were investigated by high-resolution fluorescence spectroscopy in physiological salt solutions, in the presence and absence of 100 nmol/L Ca^{2+}. The $\lambda_{ex\text{-}max}$ for Be^{2+}, Ca^{2+}, Ba^{2+}, Sr^{2+}, and La^{3+} in the absence of Ca^{2+} was 354, 310, 320, 317, and 316 nm, respectively. The optimal $\lambda_{em\text{-}max}$ for all divalent cations in Ca^{2+} free buffer was 502$\pm$8 nm. Individual spikes were obtained by sequential irradiation at 340 and 380 nm, respectively, and the intensity ratios compared with nonspiked Ca^{2+} containing buffer. These experiments revealed a minor competition by 100 nmol/L Ca^{2+} for fura-2 binding sites in the series Ba^{2+}, Sr^{2+}, and La^{3+}. However, Ca^{2+} competed strongly against Be^{2+}, resulting in an $\approx$60% decrease in the 340-nm signal and a 4% increase in the 380-nm signal vis-à-vis other cations[2+3+].

We performed molecular modeling experiments to ascertain structural differences between fura-Be^{2+} and other fura-cation[2+3+] that may account for the measurable difference in complex excitation wavelengths. The uncomplexed fura ground state structure resembles a glove-like pocket with preferential cation[2+3+] binding to the carboxylates extending from the 5-carboxy-oxazolyl and one of the *N*-acetyl-5-methylphenoxy moieties, respectively (Figure 2). In the fura-2-cation complexes involving Ca^{2+}, Mg^{2+}, Sr^{2+}, and La^{3+}, a relatively planar extended π-conjugated network involving the oxazolyl- and benzofuranyloxy-rings were observed, with minor deviance from overall planarity (0.68°). However, Be^{2+} complexation significantly distorted the fura π conjugated network (25.32°), shifting the excitation spectrum. Indeed, the molecular backbone in the fura-Be^{2+} complex is distorted from planarity (twisted). In contrast, when compared with one another, fura complexes with Ca^{2+}, Mg^{2+},

Sr^{2+}, and La^{3+} have only a 0.68° deviance from planarity (coplanar). These findings are consistent with the idea that backbone distortion unmasks an unusual $\lambda_{ex\text{-}max}$ in the presence of Ca^{2+} (eg, 2 mm Be^{2+} bathchromically shifts the fura spectrum a longer wavelength).

Using parameters established in vitro to optimize cation-fura fluorescence, thapsigargin-induced ion permeability was evaluated in PAECs and PMVECs. In low extracellular Ca^{2+}, thapsigargin promoted Ca^{2+} release from intracellular stores that transiently increased $[Ca^{2+}]_i$. Readdition of extracellular Ca^{2+} resulted in an abrupt $[Ca^{2+}]_i$ rise that was larger in PAECs than in PMVECs (Figure 3A), compatible with previous recalcification studies in these cells.[1,7] Similar experiments using Be^{2+}, Sr^{2+} and Ba^{2+} cations in the reentry protocol revealed thapsigargin activated identical nonselective $[cation]_i$ responses in PAECs and PMVECs (Figure 3B).

To establish relative permeability ratios to divalent cations in PAECs and PMVECs, thapsigargin-induced cation entry was compared with digitonin-induced cation entry.[24] Digitonin permeabilizes cell membranes and thus promotes cation equilibration between extracellular and intracellular compartments. Digitonin did not stimulate Ca^{2+} release from intracellular stores (Figure 3C), indicating the endoplasmic reticulum membrane was not permeabilized. Addition of Ca^{2+}, Be^{2+}, Ba^{2+}, and Sr^{2+} each abruptly increased $[cation]_i$ in PAECs and PMVECs (Figure 3C and 3D). Whereas the $[Be^{2+}]_i$, $[Ba^{2+}]_i$, and $[Sr^{2+}]_i$ responses to digitonin were stable (data not shown), the $[Ca^{2+}]_i$ response reached a peak level that slowly decreased to a plateau. These findings suggest Ca^{2+} reuptake into intracellular stores and extrusion across the plasma membrane remained active. Collectively, digitonin-induced $[cation]_i$ responses were similar in PAECs and PMVECs.

Establishing a ratio between thapsigargin- and digitonin-induced $[cation]_i$ responses allows for direct assessment of the cation permeability pathways that are stimulated after Ca^{2+} store depletion. These findings resolve that thapsigargin activates a nonselective cation entry pathway in PMVECs with a relative permeability ratio of $Be^{2+}>Ba^{2+}>Sr^{2+}>Ca^{2+}$. In contrast, Ca^{2+} permeability is higher in PAECs (0.28) than it is in PMVECs (0.17), suggesting either Ca^{2+} permeates
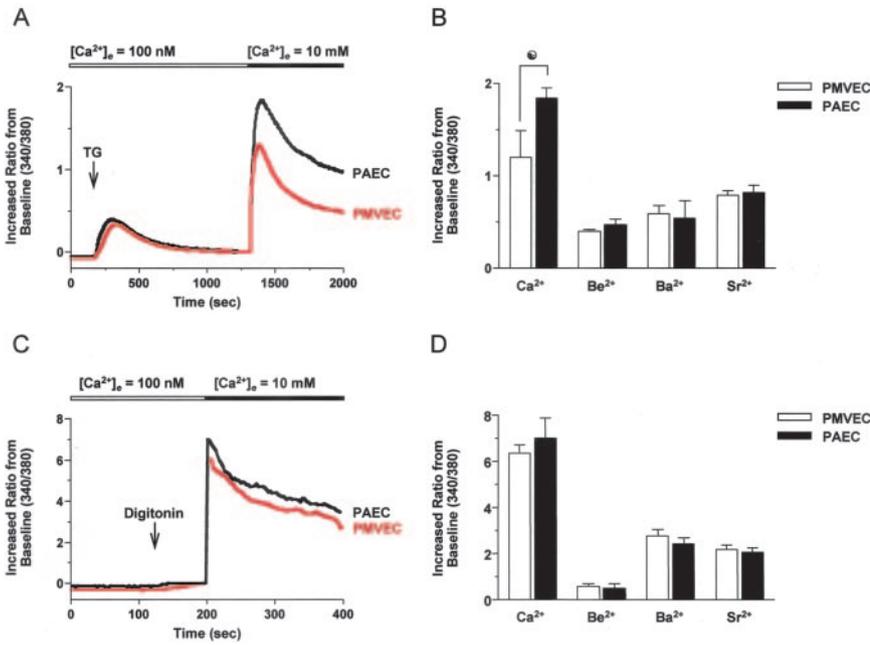
Figure 3. PAECs possess a SOC entry pathway that is not normally present in PMVECs. A, Fura-loaded cells were incubated in 100 nmol/L Ca^{2+} Ringer's solution designed to clamp membrane potential in intact cells and exposed to 1 μmol/L thapsigargin (TG). Thapsigargin stimulated Ca^{2+} release from intracellular stores and transiently increased $[Ca^{2+}]_i$. Subsequent media recalcification ($[Ca^{2+}]_e$) promoted SOC entry that was greater in PAECs than in PMVECs. B, Recalcification studies using Be^{2+}, Sr^{2+}, and Ba^{2+} revealed identical cation entry in PAECs and PMVECs (*$P<0.05$). C, Nonspecific cation entry was examined using a similar protocol. Digitonin (1 μmol/L) was applied to permeabilize the plasma membrane, and then Ca^{2+} was replenished to the extracellular media. Similar $[Ca^{2+}]_i$ rises were observed in PAECs and PMVECs. D, Be^{2+}, Ba^{2+}, and Sr^{2+} entry through digitonin permeabilized membranes was also similar in both cell types.

nonselective channels more efficiently in PAECs or, alternatively, thapsigargin activates a Ca^{2+}-selective entry pathway in PAECs that is not activated in PMVECs.

La^{3+} permeates ion channels and can inhibit Ca^{2+} entry by an "intracellular" block,[25] perhaps because the effective ionic radii of the solvated octahedrally coordinated ions are remarkably similar ($Ca^{2+}=1.00$ Å; $La^{3+}=1.05$ Å).[26] This size similarity is a consequence of the well-known "lanthanide contraction," ie, the poor shielding by the outer valence electrons in the 4th and 5th subshell levels results in an increase in the effective nuclear charge and thus a concomitant reduction in ionic size.[27] We investigated thapsigargin-activated La^{3+} permeability and compared this permeability to Ca^{2+}. La^{3+} permeability was equal in PAECs (0.28) and PMVECs (0.27) (Figure 4) and was nearly identical to the Ca^{2+} permeability observed in PAECs (0.28). However, in PMVECs, La^{3+} permeability was higher than that of Ca^{2+}, suggesting La^{3+} influx occurs through a Ca^{2+} impermeable pore or, alternatively, that it more readily accesses a Ca^{2+} permeable pore. Ion-water interaction is an important determinant of ion permeability through the pores of ion channels,[28,29] where water is excluded from the channel's internal pore. To the extent that the ions are solvated in an aqueous medium, it has been suggested that ion-water complexes are most stable when the electronegativity of the water ligands was such that the cation achieved an essentially neutral condition (electroneutrality principle).[30,31] Accordingly, Be^{2+} forms a tetrahedral aqueous complex, whereas Ca^{2+}, Mg^{2+}, Sr^{2+}, Ba^{2+}, and La^{3+} all form stable octahedral aqueous complexes. Qualitatively, the degree of hydration of a metal complex mediates the availability of electron density and resultant ionic charge of the metal centers themselves. Although the solvated ion-complex has a net formal charge of either $+2$ (Ca^{2+}) or $+3$ (La^{3+}), the net positive charges are dispersed over the 12 hydrogen atoms of the solvated complexes. The removal of water ligands as the ion is desolvated for passage through the ion pore, and resolvated on intracellular entry, introduces complex charge interactions between the free ion and the transmembrane protein amino acids themselves. La^{3+} that dissociates from water as it enters the ion pore may have more favorable charge-contact interactions and charge stabilization and thus permeate a partially closed or inactivated channel more readily than would Ca^{2+}. This suggests that La^{3+} may more readily access a Ca^{2+} permeable pore in PMVECs.

I_{SOC} Activation in Endothelial Cells
Conduit endothelial cells possess a thapsigargin-activated Ca^{2+}-selective current, I_{SOC}.[13–15] We therefore sought to determine whether the decrease in thapsigargin-induced Ca^{2+}
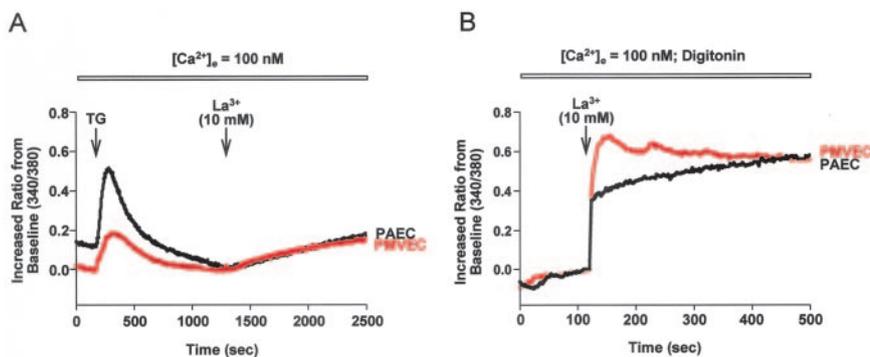

Figure 4. La^{3+} similarly permeates SOC entry channels in PAECs and PMVECs. A, Fura-loaded cells were incubated in 100 nmol/L Ca^{2+} Ringer's solution, thapsigargin (TG; 1 μmol/L) was applied to activate SOC entry channels, and La^{3+} replenished to the extracellular media. La^{3+} entry through SOC entry channels was similar between PAECs and PMVECs. B, La^{3+} entry was also similar in PAECs and PMVECs after membrane permeabilization using digitonin (1 μmol/L).
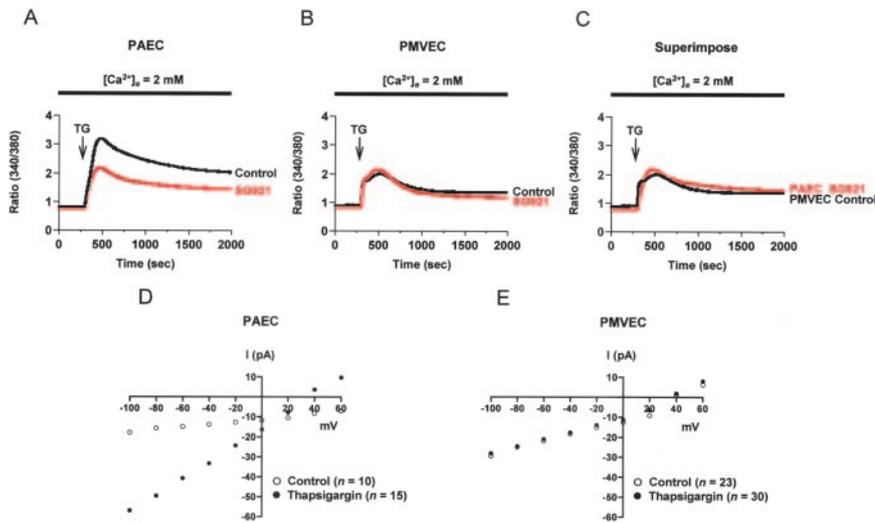
Figure 5. Thapsigargin activates a Ca^{2+}-selective entry pathway (I_{SOC}) in PAECs that is not typically activated in PMVECs. A, Experiments were performed using PAECs grown to confluence on Cellocate coverslips and microinjected with either PBS or 70 μg/mL of an antibody (SG921) to disrupt the spectrin-protein 4.1 interaction. Thapsigargin (TG; 1 μmol/L) stimulates a slowly developing, sustained rise in $[Ca^{2+}]_i$. Disruption of the spectrin-protein 4.1 interaction decreases the thapsigargin $[Ca^{2+}]_i$ response by $\approx$40%. B, Similar experiments using PMVECs demonstrate these cells do not possess a thapsigargin-activated SOC entry pathway that requires a spectrin-protein 4.1 interaction. C, Overlay of the thapsigargin-induced $[Ca^{2+}]_i$ responses in PAECs, following disruption of the spectrin-protein 4.1 interaction, and PMVECs demonstrates microvascular cells do not possess the SOC entry pathway regulated by the spectrin-protein 4.1 interaction. D, Single cells were isolated in a whole-cell voltage clamp mode, as described previously.[14,15] Current-voltage relationships were recorded 3 to 5 minutes after break-in. Two hundred–millisecond pulses were applied every 3 seconds, from −100 to +60 mV, with 20-mV increments; the holding potential was 0 mV. In PAECs, thapsigargin (1 μmol/L) application through the patch pipette activated a small inward Ca^{2+} current characteristic of I_{SOC}. E, However, in PMVECs, thapsigargin did not activate I_{SOC}, indicating the microvascular cells normally lack this Ca^{2+}-selective current.

permeability in PMVECs resulted from an apparent absence of I_{SOC}. I_{SOC} activation requires interaction between spectrin and protein 4.1.[15] Figure 5A illustrates, as in our earlier studies,[15] that disruption of the spectrin-protein 4.1 interaction, done by using a spectrin antibody SG921 that specifically targets on protein 4.1 binding domain on spectrin, reduces the global $[Ca^{2+}]_i$ response to thapsigargin by $\approx$40% in PAECs. However, disruption of the spectrin-protein 4.1 interaction did not alter the global $[Ca^{2+}]_i$ response to thapsigargin in PMVECs (Figure 5B). Superimposition of thapsigargin-induced $[Ca^{2+}]_i$ responses from PAECs after disruption of spectrin-protein 4.1 binding and "normal" PMVECs revealed an exact overlay (Figure 5C), suggesting microvascular endothelial cells lack I_{SOC}. To address this issue further, thapsigargin was applied to single PAECs and PMVECs in a conventional whole-cell configuration using solutions previously described.[14,15] In PAECs, thapsigargin activated an inward Ca^{2+} current ($\approx$60 pA on average) that reversed near +40 mV and was inwardly rectifying (Figure 5D). In PMVECs, thapsigargin did not activate an inward current despite repeated efforts (Figure 5E), again suggesting microvascular endothelial cells lack I_{SOC}.

Endothelial cells isolated from TRPC4-deficient mice lack I_{SOC},[32] and antisense inhibition of TRPC1 reduces I_{SOC}.[14] These findings have been taken as support for the idea that TRPC1 and TRPC4 proteins form—at least in part—the molecular basis of I_{SOC} channels in endothelial cells.[13,14] If this idea is correct and PMVECs lack I_{SOC}, then these cells should not express TRPC1 or TRPC4. We examined TRPC4 expression in PMVECs and found it to be prominently expressed, as in PAECs (Figure 6A). As in our studies using PAECs, the PMVEC TRPC4 channel is physically associated with protein 4.1 (data not shown). Thus, it appears PMVECs possess the molecular machinery necessary to activate I_{SOC}.

The type 6 calcium-inhibited adenylyl cyclase, AC6, is expressed in both PAECs and PMVECs. Although submicro-

molar calcium concentrations inhibit AC6 activity in membranes isolated from both cell types,[33,34] calcium inhibition of whole-cell cAMP is difficult to resolve in PMVECs.[18,33] Preincubation of PMVECs with rolipram elevates cAMP dramatically, and unmasks calcium inhibition of cAMP synthesis.[33] We therefore questioned whether rolipram reveals a thapsigargin-activated I_{SOC}, providing the calcium source that regulates AC6 activity. Rolipram treatment unmasked the I_{SOC} current in PMVECs (Figure 6B), suggesting I_{SOC} channels exist near AC6 and importantly control enzyme activity. However, rolipram treatment abolished I_{SOC} in PAECs (Figure 6C), underscoring the distinct role of phosphodiesterase 4 in regulating membrane cAMP concentrations, and actions, in PAECs and PMVECs.

I_{SOC} in Control of PMVEC Permeability

SOC entry is sufficient to induce gaps in endothelial cells derived from conduit vessels, but not in endothelial cells isolated from the microcirculation.[1,5] We questioned whether the absence of I_{SOC} in PMVECs contributes to their insensitivity to thapsigargin. Figure 7A and the accompanying time-compressed video shows the stable junctional apposition in PMVECs (see Online Movies 1 and 2 in the online data supplement available at http://circres.ahajournals.org). However, pretreatment with rolipram reveals thapsigargin-induced gap formation, consistent with the idea that Ca^{2+} permeation through I_{SOC} channels disrupt cell-cell and cell-matrix tethering and increase centripetally directed tension sufficient to form an intercellular gap.

We examined the relevance of I_{SOC} activation in the pulmonary circulation. Thapsigargin increased lung permeability $\approx$3-fold, estimated by filtration coefficient (Figure 7B). Lung perfusion casts revealed prominent endothelial cell leak sites in extra-alveolar vessels, but evidence for increased permeability was not resolved in capillary segments (Figure 7C). Rolipram pretreatment decreased the thapsigargin-
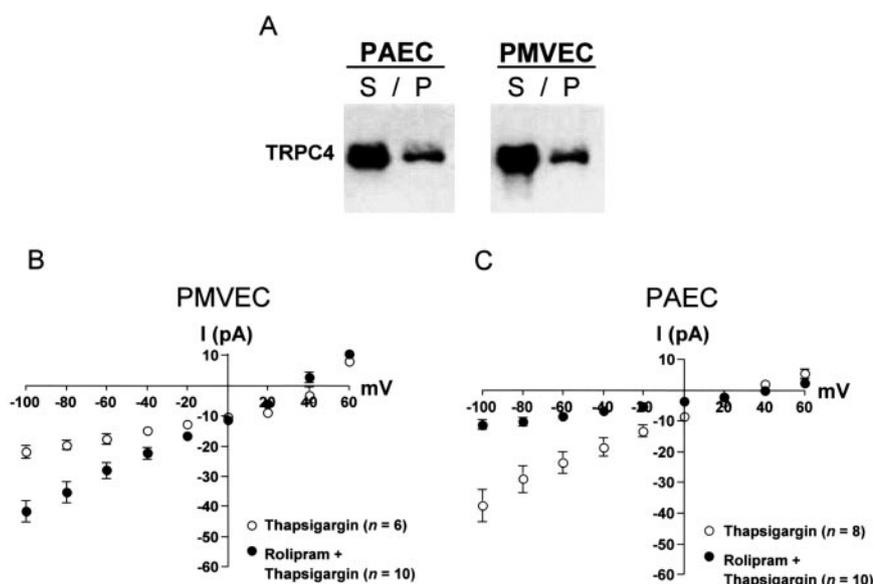
Figure 6. PMVECs express TRPC4 and can be induced to activate I_{SOC}. A, PMVEC monolayers were lysed, and the membrane skeleton extracted using Triton-X 100 with 100 mmol/L potassium iodide (KI). Immunoblot analysis of Triton-X insoluble (P) and soluble (S) fractions revealed TRPC4 (approximately 110 kDa) was located predominately in the S fraction. TRPC4 was found with protein 4.1 ($\approx$110 kDa) (data not shown). B, Single cells were incubated with the type 4 phosphodiesterase inhibitor, rolipram, and a whole-cell voltage clamp configuration established as described elsewhere.[14,15] Two hundred–millisecond pulses were applied every 3 seconds, from -100 to $+60$ mV, with 20-mV increments; the holding potential was 0 mV. Whereas thapsigargin (TG; 1 μmol/L) alone did not activate I_{SOC}, rolipram (10 μmol/L) pretreatment revealed I_{SOC} activation. C, In contrast, thapsigargin (1 μmol/L) was sufficient to activate I_{SOC} in PAECs, whereas rolipram (10 μmol/L) pretreatment abolished the current.

induced rise in permeability by nearly 50%. However, whereas rolipram decreased gap formation in extra-alveolar vessels, it increased permeability across capillary segments (Figure 7D). Thus, the net effect of the rolipram/thapsigargin treatment was to diminish leak sites in extra-alveolar vessels and to open new leak sites in the microcirculation, consistent with a role for I_{SOC} activation in formation of interendothelial cell gaps.

Discussion

Thapsigargin elevates $[Ca^{2+}]_i$ by simultaneously activating multiple SOC entry pathways. Both Ca^{2+}-selective and nonselective cation entry pathways can be discriminated electrophysiologically,[13] but commonly the molecular basis of the channel that underlies this current and its relation to endothelial cell barrier function is poorly understood. Our present studies used different endothelial cell phenotypes to provide the first direct evidence that I_{SOC} activation is sufficient to increase endothelial cell permeability.

Historically endothelial cells from conduit origins, eg, aorta and pulmonary artery, have been used as models for endothelial cell function. However, it is now clear that endothelial cells along the vascular tree are phenotypically distinct based on environmental and epigenetic control of their behavior,[19] including dynamic regulation of Ca^{2+} transitions.[1,18,21,35,36] Thapsigargin activates a larger SOC entry response in PAECs than in PMVECs, although the mechanism for this observation is not clear. To discern the SOC entry pathways in PAECs and PMVECs, divalent cation entry was examined in intact cells. Three lines of evidence indicate that thapsigargin does not typically activate a Ca^{2+}-selective SOC entry pathway in PMVECs that is present in PAECs. First, in vivo recalcification studies revealed a lower Ca^{2+} permeability in PMVECs than in PAECs. Second, the global $[Ca^{2+}]_i$ response to thapsigargin was not reduced by disruption of the spectrin-protein 4.1 interaction in PMVECs, as it

was in PAECs. Third, thapsigargin did not activate I_{SOC} in PMVEC patch clamp studies. Interestingly, PMVECs express TRPC4, the protein most likely responsible for I_{SOC} activation in endothelial cells,[32,37] suggesting PMVECs lack an activation mechanism.

Rolipram pretreatment revealed the thapsigargin-activated I_{SOC} in PMVECs. The PMVEC current was activated without a change in the global $[Ca^{2+}]_i$ response to thapsigargin.[33] These findings suggest that I_{SOC} activation generates a membrane-delimited $[Ca^{2+}]_i$ pool, without changing ionic concentrations in the bulk cytosolic compartment. Indeed, membrane-associated $[Ca^{2+}]$ is constitutively higher than bulk cytosolic $[Ca^{2+}]$.[38,39] Recent work by Isshiki and colleagues[38,40] supports this idea. In their studies, a subcortical $[Ca^{2+}]$ pool was distinguishable from bulk cytosolic and mitochondrial $[Ca^{2+}]$ sources. Subcortical $[Ca^{2+}]$ specifically controlled nitric oxide production and PKCβ translocation, without altering PLA$_2$ activation. Our group has similarly shown that Ca^{2+} transitions through endothelial cell "leak" channels inhibit basal cAMP production without dramatically altering global $[Ca^{2+}]_i$.[34] Thus, it is not surprising that the activation of a small, Ca^{2+}-selective current impacts membrane events without a change in bulk cytosolic function.

Although rolipram revealed the I_{SOC} in PMVECs, it inhibited the thapsigargin-induced current in PAECs, allowing us to use rolipram as a tool to examine the importance of this current in controlling endothelial barrier function. In both cell types, the appearance of I_{SOC} was required for thapsigargin to disrupt junctional apposition and decrease barrier function. However, this phenomenon was most pronounced in the intact lung, where rolipram treatment "shifted" the thapsigargin-induced leak site from extra-alveolar vessels to capillary segments, in accordance with site-specific I_{SOC} activation. Thus, rolipram desensitized extra-alveolar endothelium, and sensitized the alveolar endothelium, to Ca^{2+} transitions through I_{SOC}.
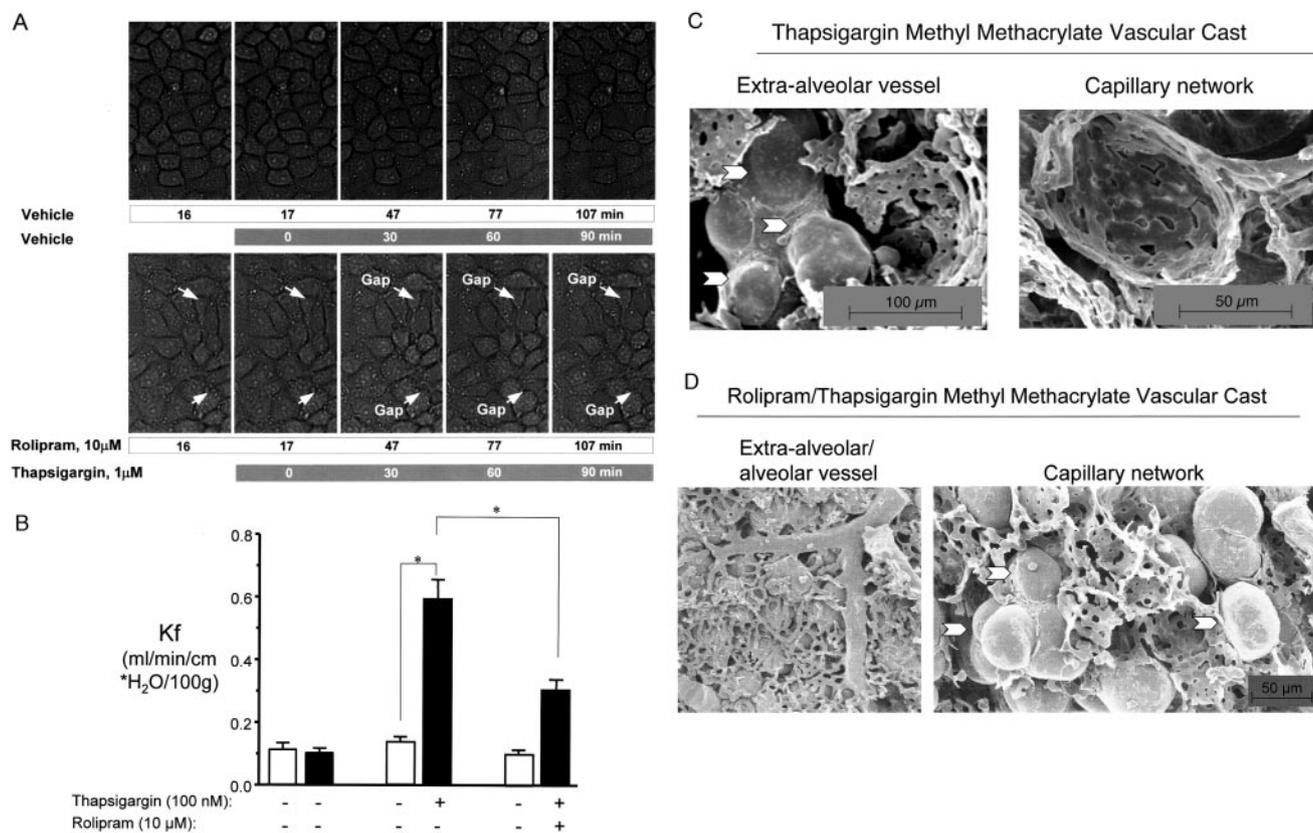
Figure 7. I_{SOC} provides a $[Ca^{2+}]_i$ source that is needed for thapsigargin to increase PMVEC permeability. A, PMVEC junctional apposition is stable in confluent monolayers (see online Movies). However, pretreatment with 10 μmol/L rolipram unmasks thapsigargin-induced intercellular gap formation in PMVECs (see online Movies), indicating I_{SOC} provides a $[Ca^{2+}]_i$ source needed for intercellular gap formation. B, Kf was measured before (□) and 20 minutes after (■) addition of thapsigargin (100 nmol/L) or vehicle control. Whereas thapsigargin increased Kf ≈ 3-fold, rolipram pretreatment attenuated this rise in permeability (*$P<0.05$). C, Lung vascular corrosion casts reveal thapsigargin-induced leak sites in the pulmonary circulation. After lungs were isolated and perfused, baseline Kf measurements were made before (0.19±0.03 mL/min/cm H_2O per 100g) and after (0.69±0.12 mL/min/cm H_2O per 100g) thapsigargin (100 nmol/L) application. Venous pressure was then raised by ≈8 cm H_2O from baseline, and a prepolymerized methyl methacrylate solution was circulated as described (see Materials and Methods). SEM of vascular casts reveals that thapsigargin induces leak sites in extra-alveolar blood vessels, and not in capillary segments. Data are representative of results from 4 separate experiments. Arrows denote sites where the casting material exits the circulation. D, Rolipram (10 μmol/L) pretreatment decreased the Kf response to thapsigargin (100 nmol/L; 0.45±0.12 mL/min/cm H_2O per 100g; n=3). After final Kf measurements, lung corrosion casts were generated and examined by SEM as described in C. Rolipram/thapsigargin-treated lungs exhibited a decrease in extra-alveolar leak sites and a striking increase in permeability across capillary segments. Arrows denote sites where the casting material exits the circulation.

The mechanisms responsible for these discrete rolipram actions are unknown. Rolipram increases cAMP concentrations in both cell types, although to a greater extent in PMVECs.[7,18,33] PMVECs exhibit a high cAMP turnover rate due to high membrane-associated phosphodiesterase 4 activity.[33] Phosphodiesterase activity importantly targets cAMP to effector molecules and fulfills a central role in achieving the threshold concentrations that are necessary to activate appropriate PKA and Epac molecules.[41] Although rises in membrane cAMP protect the microvascular endothelial cell barrier,[18] cAMP fluxes occurring outside this domain disrupt the endothelial cell barrier.[22] Thus, although speculative, rolipram may allow cAMP to escape its membrane domain in PMVECs and, when combined with I_{SOC} activation that reduces membrane cAMP, result in loss of cell-cell apposition. Future studies will be required to examine how the rolipram and thapsigargin treatments discretely control $[Ca^{2+}]$ and cAMP pools to regulate PMVEC barrier function.

In conclusion, we have demonstrated that PAECs and PMVECs possess different signaling pathways that control their SOC entries. Whereas thapsigargin activates I_{SOC} in PAECs, it does not typically activate I_{SOC} in PMVECs. However, the phosphodiesterase 4 inhibitor, rolipram, reveals the thapsigargin-activated I_{SOC} in PMVECs and, most importantly, sensitizes alveolar endothelium to Ca^{2+} transitions that lead to pulmonary edema. These results must be considered as potential complications to the clinical utility of rolipram and related phosphodiesterase inhibitors.[42,43]

Acknowledgments

References

1. Kelly JJ, Moore TM, Babal P, Diwan AH, Stevens T, Thompson WJ. Pulmonary microvascular and macrovascular endothelial cells: differ-

ential regulation of Ca^{2+} and permeability. *Am J Physiol*. 1998;274: L810–L819.

2. Moore TM, Brough GH, Babal P, Kelly JJ, Li M, Stevens T. Store-operated calcium entry promotes shape change in pulmonary endothelial cells expressing Trp1. *Am J Physiol*. 1998;275:L574–L582.

3. Moore TM, Norwood NR, Creighton JR, Babal P, Brough GH, Shasby DM, Stevens T. Receptor-dependent activation of store-operated calcium entry increases endothelial cell permeability. *Am J Physiol Lung Cell Mol Physiol*. 2000;279:L691–L698.

4. Alvarez DF, King JA, Townsley MI. Evaluation of endothelial permeability by a corrosion casting technique. *Microsc Microanal*. 2004;10: 200–201.

5. Chetham PM, Babal P, Bridges JP, Moore TM, Stevens T. Segmental regulation of pulmonary vascular permeability by store-operated Ca^{2+} entry. *Am J Physiol*. 1999;276:L41–L50.

6. Parker JC, Yoshikawa S. Vascular segmental permeabilities at high peak inflation pressure in isolated rat lungs. *Am J Physiol Lung Cell Mol Physiol*. 2002;283:L1203–L1209.

7. Stevens T, Creighton J, Thompson WJ. Control of cAMP in lung endothelial cell phenotypes. Implications for control of barrier function. *Am J Physiol*. 1999;277:L119–L126.

8. Nilius B, Viana F, Droogmans G. Ion channels in vascular endothelium. *Annu Rev Physiol*. 1997;59:145–170.

9. Nilius B, Droogmans G. Ion channels and their functional role in vascular endothelium. *Physiol Rev*. 2001;81:1415–1459.

10. Nilius B, Droogmans G, Wondergem R. Transient receptor potential channels in endothelium: solving the calcium entry puzzle? *Endothelium*. 2003;10:5–15.

11. Fasolato C, Nilius B. Store depletion triggers the calcium release-activated calcium current (ICRAC) in macrovascular endothelial cells: a comparison with Jurkat and embryonic kidney cell lines. *Pflugers Arch*. 1998;436:69–74.

12. Vaca L, Kunze DL. Depletion of intracellular Ca^{2+} stores activates a Ca^{2+}-selective channel in vascular endothelium. *Am J Physiol*. 1994;267: C920–C925.

13. Cioffi DL, Wu S, Stevens T. On the endothelial cell I(SOC). *Cell Calcium*. 2003;33:323–336.

14. Brough GH, Wu S, Cioffi D, Moore TM, Li M, Dean N, Stevens T. Contribution of endogenously expressed Trp1 to a Ca^{2+}-selective, store-operated Ca^{2+} entry pathway. *FASEB J*. 2001;15:1727–1738.

15. Wu S, Sangerman J, Li M, Brough GH, Goodman SR, Stevens T. Essential control of an endothelial cell ISOC by the spectrin membrane skeleton. *J Cell Biol*. 2001;154:1225–1233.

16. Kamouchi M, Philipp S, Flockerzi V, Wissenbach U, Mamin A, Raeymaekers L, Eggermont J, Droogmans G, Nilius B. Properties of heterologously expressed hTRP3 channels in bovine pulmonary artery endothelial cells. *J Physiol*. 1999;518:345–358.

17. Wu S, Moore TM, Brough GH, Whitt SR, Chinkers M, Li M, Stevens T. Cyclic nucleotide-gated channels mediate membrane depolarization following activation of store-operated calcium entry in endothelial cells. *J Biol Chem*. 2000;275:18887–18896.

18. Cioffi DL, Moore TM, Schaack J, Creighton JR, Cooper DM, Stevens T. Dominant regulation of interendothelial cell gap formation by calcium-inhibited type 6 adenylyl cyclase. *J Cell Biol*. 2002;157:1267–1278.

19. Gebb S, Stevens T. On lung endothelial cell heterogeneity. *Microvasc Res*. 2004;68:1–12.

20. King J, Hamil T, Creighton J, Wu S, Bhat P, McDonald F, Stevens T. Structural and functional characteristics of lung macro- and microvascular endothelial cell phenotypes. *Microvasc Res*. 2004;67:139–151.

21. Wu S, Haynes J Jr, Taylor JT, Obiako BO, Stubbs JR, Li M, Stevens T. Cav3.1 (alpha1G) T-type Ca^{2+} channels mediate vaso-occlusion of sickled erythrocytes in lung microcirculation. *Circ Res*. 2003;93: 346–353.

22. Sayner SL, Frank DW, King J, Chen H, VandeWaa J, Stevens T. Paradoxical cAMP-induced lung endothelial hyperpermeability revealed by Pseudomonas aeruginosa ExoY. *Circ Res*. 2004;95:196–203.

23. Gannon BJ. Preparation of microvascular corrosion media: procedure for partial polymerization of methyl metacrylate using ultraviolet light. *Biom Res*. 1981;2:227–233.

24. Zweifach A. Target-cell contact activates a highly selective capacitative calcium entry pathway in cytotoxic T lymphocytes. *J Cell Biol*. 2000; 148:603–614.

25. Halaszovich CR, Zitt C, Jungling E, Luckhoff A. Inhibition of TRP3 channels by lanthanides. Block from the cytosolic side of the plasma membrane. *J Biol Chem*. 2000;275:37423–37428.

26. Shannon RD, Prewitt CT. Revised values of effective ionic radii. *Acta Crystallogr*. 1970;B26:1046–1048.

27. Yocum PN. Lanthanide/Actinide Chemistry. In: Gould RF, ed. *Advances in Chemistry Series*. Washington D.C.: American Chemical Society; 1967:51.

28. Doyle DA, Morais Cabral J, Pfuetzner RA, Kuo A, Gulbis JM, Cohen SL, Chait BT, MacKinnon R. The structure of the potassium channel: molecular basis of K$^+$ conduction and selectivity. *Science*. 1998;280: 69–77.

29. Pottosin II, Andjus PR, Vucelic D, Berestovsky GN. Effects of D2O on permeation and gating in the Ca^{2+}-activated potassium channel from Chara. *J Membr Biol*. 1993;136:113–124.

30. Pauling L. *The Nature of the Chemical Bond*, 3rd ed. Ithaca, NY: Cornell University Press; 1960.

31. Dunn TM. Covalency and the iron group of complexes. *J Chem Soc*. 1959;125:623–627.

32. Freichel M, Suh SH, Pfeifer A, Schweig U, Trost C, Weissgerber P, Biel M, Philipp S, Freise D, Droogmans G, Hofmann F, Flockerzi V, Nilius B. Lack of an endothelial store-operated Ca^{2+} current impairs agonist-dependent vasorelaxation in TRP4−/− mice. *Nat Cell Biol*. 2001;3: 121–127.

33. Creighton JR, Masada N, Cooper DM, Stevens T. Coordinate regulation of membrane cAMP by Ca^{2+}-inhibited adenylyl cyclase and phosphodiesterase activities. *Am J Physiol Lung Cell Mol Physiol*. 2003;284: L100–L107.

34. Stevens T, Nakahashi Y, Cornfield DN, McMurtry IF, Cooper DM, Rodman DM. Ca^{2+}-inhibitable adenylyl cyclase modulates pulmonary artery endothelial cell cAMP content and barrier function. *Proc Natl Acad Sci U S A*. 1995;92:2696–2700.

35. Stevens T, Fouty B, Hepler L, Richardson D, Brough G, McMurtry IF, Rodman DM. Cytosolic Ca^{2+} and adenylyl cyclase responses in phenotypically distinct pulmonary endothelial cells. *Am J Physiol*. 1997;272: L51–L59.

36. Stevens T, Thompson WJ. Regulation of pulmonary microvascular endothelial cell cyclic adenosine monophosphate by adenylyl cyclase: implications for endothelial barrier function. *Chest*. 1999;116:32S–33S.

37. Freichel M, Vennekens R, Olausson J, Hoffmann M, Muller C, Stolz S, Scheunemann J, Weissgerber P, Flockerzi V. Functional role of TRPC proteins in vivo: lessons from TRPC-deficient mouse models. *Biochem Biophys Res Commun*. 2004;322:1352–1358.

38. Isshiki M, Ying YS, Fujita T, Anderson RG. A molecular sensor detects signal transduction from caveolae in living cells. *J Biol Chem*. 2002;277: 43389–43398.

39. Marsault R, Murgia M, Pozzan T, Rizzuto R. Domains of high Ca2+ beneath the plasma membrane of living A7r5 cells. *EMBO J*. 1997;16: 1575–1581.

40. Isshiki M, Mutoh A, Fujita T. Subcortical Ca^{2+} waves sneaking under the plasma membrane in endothelial cells. *Circ Res*. 2004;95:e11–e21.

41. Insel PA. Location, location, location. *Trends Endocrinol Metab*. 2003; 14:100–102.

42. Dyke HJ, Montana JG. Update on the therapeutic potential of PDE4 inhibitors. *Expert Opin Investig Drugs*. 2002;11:1–13.

43. Zhu J, Mix E, Winblad B. The antidepressant and antiinflammatory effects of rolipram in the central nervous system. *CNS Drug Rev*. 2001;7:387–398.

Circulation Research

Essential Role of a Ca^{2+}-Selective, Store-Operated Current (I_{SOC}) in Endothelial Cell Permeability: Determinants of the Vascular Leak Site

Songwei Wu, Eugene A. Cioffi, Diego Alvarez, Sarah L. Sayner, Hairu Chen, Donna L. Cioffi, Judy King, Judy R. Creighton, Mary Townsley, Steven R. Goodman and Troy Stevens

The online version of this article, along with updated information and services, is located on the
World Wide Web at:
http://circres.ahajournals.org/content/96/8/856

Data Supplement (unedited) at:
http://circres.ahajournals.org/content/suppl/2005/06/06/01.RES.0000163632.67282.1f.DC1
http://circres.ahajournals.org/content/suppl/2005/03/25/01.RES.0000163632.67282.1fv1.DC1